Available online at www.sciencedirect.com

ScienceDirect

Procedia Materials Science 3 (2014) 1050 – 1055

Procedia Materials Science

www.elsevier.com/locate/procedia

20th European Conference on Fracture (ECF20)

Modeling the cold formability of dualphase steels on different length scales

Sebastian Münstermann[a]*, Junhe Lian[a], Napat Vajragupta[a]

[a] *RWTH Aachen University, Department of Ferrous Metallurgy, Intzestraße 1, 52072 Aachen, Germany*

Abstract

Modern multiphase steels contain constituents of distinctive mechanical properties, so that they develop strong gradients in the local strain distribution during forming operations and this strongly promotes the microstructural damage evolution. Consequently, the material´s resistance against ductile crack initiation sets the limits of cold formability and these can even be reached without any macroscopic necking phenomena. The modified Bai Wierzbicki (MBW) model has been proven the capability of providing an impressive accuracy of simulation results when applied to stretch forming tests as it describes ductile crack initiation and propagation. The consideration of the third invariant of the stress deviator on plasticity and ductile failure is a key factor for the model´s high accuracy, but due to its phenomenological character its applicability for materials design is currently not given. Furthermore, the quantity of material parameters is so high that an industrial application of this model cannot be expected. Therefore the paper presents an alternative approach for parameter calibration relying on virtual experiments on representative volume elements, where the plastic strain localization theory is applied without any other damage model.

Selection and peer-review under responsibility of the Norwegian University of Science and Technology (NTNU), Department of Structural Engineering

Keywords: cold formability, multiphase steels, MBW model, modelling on different length scales

1. Introduction

The cold formability of steel for automotive application has been characterized by forming limit curves (FLC) for decades. This criterion characterizes necking phenomena by providing the critical principal strains in the sheet plane

* Corresponding author. Tel.: +49 241 - 8025422; fax:+49 241 - 8092253.
E-mail address: muenstermann@iehk.rwth-aachen.de

Selection and peer-review under responsibility of the Norwegian University of Science and Technology (NTNU), Department of Structural Engineering
doi:10.1016/j.mspro.2014.06.171

Nomenclature

$c_\theta^t, c_\theta^c, c_{\theta,}^s, m$	MBW model´s material parameters for consideration of Lode angle effects on yield stress
$c_i^1, c_i^2, c_i^3, c_i^4$	MBW model´s material parameters for consideration of damage initiation
D_{crit}	critical damage
G_f	energy dissipation between damage initiation and fracture
$\bar{\varepsilon}^p$	equivalent plastic strain
$\bar{\varepsilon}^i$	equivalent plastic strain to damage initiation
$\bar{\varepsilon}^f$	equivalent plastic strain to fracture
η	stress triaxiality
$\bar{\theta}$	normalized Lode angle
σ_e	equivalent stress
σ_{yld}	yield stress
ϕ_{MBW}	yield potential of MBW model

for the instant of strain localization. The demand for resource-efficient vehicle design has led to an increased application of advanced high strength steels (AHSS) in automotive engineering but Tasan et al. (2009) observed that in these materials crack initiation can happen prior to necking. Consequently the FLC must not be used for the evaluation of forming processes anymore when modern multiphase steels are subject of investigation. The main reason for early crack initiation in multiphase steels is the development of strong gradients in the local strain distribution during forming operations, which result in significant amounts of damage on the micro scale. This also affects the sample´s macroscopic behavior when cracks are formed. Attempts to provide a fracture forming limit curve have been made in order to allow evaluating the cold formability of multiphase steels with the well-established approaches, but investigations of Chin-Chan (1982) have already earlier pointed out that the forming limit curves are strain-path dependent in general. To conclude, a tool for the numerical prediction of damage initiation during cold forming of multiphase sheet steels is required. For reasons of industrial applicability, this new approach has to fulfill strong requirements on the computational efficiency, on the reliability of results, on the number of parameters, and the scheme for parameter calibration.

Due to the requirements on the computational efficiency phenomenological ductile damage models are the favorable choice for the required model development. These models usually characterize the critical local loading conditions by providing the equivalent strain to ductile fracture as a function of parameters that describe the state of stress. Already in the 1960s, the pronounced effect of stress triaxiality on the equivalent plastic strain to ductile fracture was described, e.g. by McClintock (1968) or Rice and Tracey (1969). During the last years, also the influence of the third invariant of the stress deviator has raised the interest of the scientific community. Barsoum and Faleskog (2007), Bai and Wierzbicki (2008) and Gao et al. (2009) have proven that the normalized Lode angle, a parameter that is directly connected to the third invariant of the stress deviator, exhibits a pronounced influence on the failure strain. Since this effect is even more pronounced at comparably low stress triaxiality, it is especially important when sheet materials are investigated.

Recently, Lian et al. (2013) have presented a hybrid ductile damage model suitable to numerically describe cold forming operations of multiphase steels with a high accuracy. Their model has been strongly inspired by the work of Bai and Wierzbicki (2008), that is why their approach is called the modified Bai Wierzbicki (MBW) model. Compared to the original Bai Wierzbicki model, the MBW model is characterized by two major modifications. Firstly, the MBW model´s yield potential already evaluates the effect of ductile damage as it incorporates a damage variable D, so that the MBW model belongs to the group of coupled continuum damage mechanics models instead of uncoupled empirical failure criteria. Secondly, the MBW model´s yield potential does not consider the effect of stress triaxiality when it is applied on cold formable steels. Thus, eq. 1 presents the MBW model´s yield potential:

$$\Phi_{MBW} = \sigma_e - (1-D)\cdot\sigma_{yld}(\bar{\varepsilon}^p, \bar{\theta}) \leq 0 \quad (1).$$

Herein, the yield strength definition takes the effects of equivalent plastic strain and Lode angle parameter into consideration:

$$\sigma_{yld}(\bar{\varepsilon}^p,\bar{\theta}) = \bar{\sigma}_{yld}(\bar{\varepsilon}^p,\bar{\theta}) \cdot \left[c_\theta^s + \left(c_\theta^{ax} - c_\theta^s \right) \cdot \left(\gamma - \frac{\gamma^{m+1}}{m+1} \right) \right] \tag{2},$$

where:

$$\gamma = \frac{\frac{\sqrt{3}}{2}}{1-\frac{\sqrt{3}}{2}} \cdot \left[\frac{1}{\cos\left(\theta - \frac{\pi}{6} \right)} - 1 \right] \tag{3},$$

$$c_\theta^{ax} = \begin{cases} c_\theta^t, \text{ for } \bar{\theta} \geq 0 \\ c_\theta^c, \text{ for } \bar{\theta} < 0 \end{cases} \tag{4}.$$

The parameters $c_\theta^t, c_\theta^c, c_{\theta,}^s$ and m compensate the influences of the third invariant of the stress deviator on the material´s yield stress. They are usually calibrated in an iterative procedure that aims to find a set of material parameters showing the best agreement between numerical and experimental results. For this purpose, a series of tests is performed on samples that exhibit characteristic states of stress, namely central hole samples, notched dog bone samples, notched plane strain samples, hydraulic bulge tests. These tests initially allow calibrating the plasticity parameters. Later on, this step is followed by an adjustment of parameters describing the ductile damage evolution. For steel DP600, the process of material parameter calibration is described in detail in Lian et al. (2013).

Since the ductile failure process is characterized by the three stages of void nucleation, growth and coalescence, the MBW model´s damage evolution law consists of three criteria. Void nucleation is assumed to happen when the nucleation strain $\bar{\varepsilon}^i$ (a function of stress triaxiality and Lode angle parameter, the so-called damage initiation locus DIL) is reached. For the description of subsequent void growth, it is assumed that the energy dissipation G_f of a material point from the instant of void nucleation to the instant of complete failure is a characteristic value that can be used to express a linear damage evolution with increasing equivalent plastic strain. Finally, since void interaction effects govern the stage of void coalescence, a critical damage variable D_{crit} is introduced. Here it is assumed, that these void interaction effects begin when D_{crit} is reached. Thus, the damage evolution law reads:

$$D = \begin{cases} 0, \text{ for } \bar{\varepsilon}^p < \bar{\varepsilon}^i \\ \int_{\bar{\varepsilon}^i}^{\bar{\varepsilon}^f} \frac{L \cdot \sigma_{y,0}}{2G_f} d\bar{\varepsilon}^p, \text{ for } \bar{\varepsilon}^i \leq \bar{\varepsilon}^p \leq \bar{\varepsilon}^f \\ D_{crit}, \text{ for } \bar{\varepsilon}^f < \bar{\varepsilon}^p \end{cases} \tag{5}$$

where:

$$\bar{\varepsilon}^i = \left[c_i^1 \cdot e^{-c_i^2 \cdot \eta} - c_i^3 \cdot e^{-c_i^4 \cdot \eta} \right] \cdot \bar{\theta}^2 + \left[c_i^1 \cdot e^{-c_i^2 \cdot \eta} \right] \cdot \bar{\theta} + c_i^3 \cdot e^{-c_i^4 \cdot \eta} \tag{6}$$

Altogether, the presented MBW model contains 10 material parameters out of which 4 directly originate from the yield potential (plasticity parameters), whereas 6 parameters are used for the damage evolution law (damage evolution parameters). In some cases, it might be sufficient to apply the *von Mises* plasticity model, so that finally, only 6 parameters would have to be calibrated. Noteworthy, the decision on the plasticity model should reflect the desired accuracy of the simulation results. The subsequent chapter highlights a new approach for calibration of the four damage initiation parameters.

2. Calibration of damage initiation parameters in RVE simulations

The material under investigation is cold-rolled dualphase steel delivered in a thickness of 1.5 mm. This steel was already investigated for the study of Lian et al. (2013) where the MBW model and the conventional approach to calibrate the material parameters are discussed. Its microstructure was characterized by electron backscatter diffraction (EBSD) in order to clearly distinguish between the ferritic and the martensitic phase, fig. 1. The average martensite volume fraction turned out to be approximately 10 %.

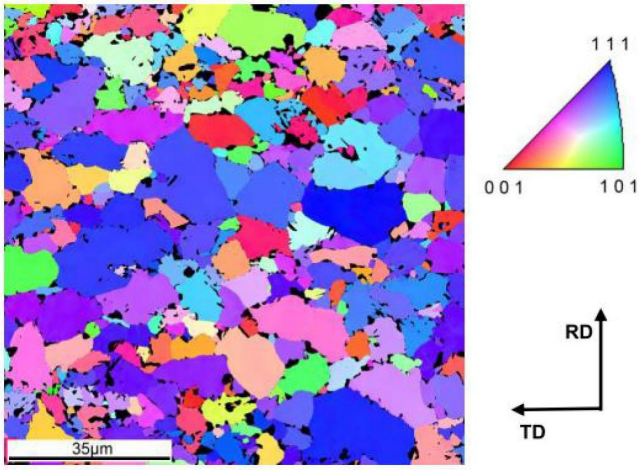

Fig. 1. Electron Back-Scattered Diffraction (EBSD) micrograph of steel DP600.

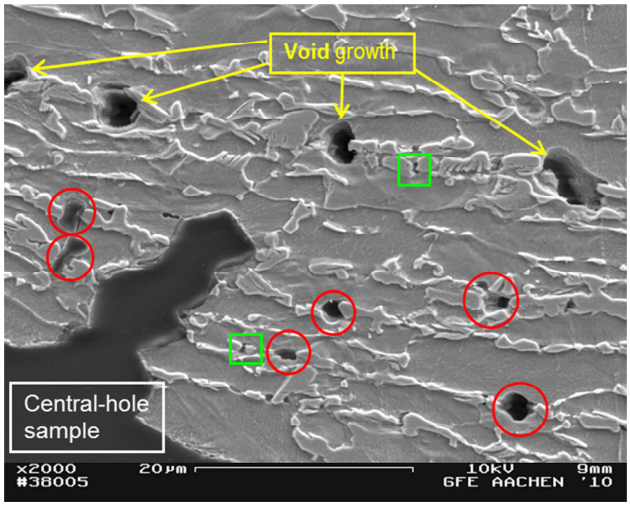

Fig. 2. Investigation of ductile damage initiation sites in steel DP600.

Specimens tested for the previous study of Lian et al. (2013) were now investigated with respect to the underlying ductile failure mechanisms. For this purpose, SEM investigations were carried out on fractured central-hole and plane-strain samples just beneath the fracture surface on through-thickness cross-sections. As it can be observed from Fig. 2, there are voids that have just nucleated at the interface between ferrite and martensite, and this process is especially fostered when two martensite islands are relatively close to each other with a small ferrite grain in between them. Additionally, a small fraction of martensite cracking is also observed.

For the construction of the RVE, a 25µm×25µm square is cut out of the EBSD micrograph. Its size reflects the characteristic length of damage initiation as experimentally observed. For the simulations, the differentiation between the ferritic and the martensitic phase is made possible by an automatic segmentation using a photo processing software. By adjusting the color threshold value, the two phases can be distinguished and a monochrome image is generated that can be transferred to Abaqus. The model assumes perfect bonding between both phases and the individual flow curves of ferrite and martensite are constructed based on an empirical model relating the Peierl´s stress to the local chemical composition. Details on this flow curve construction have been presented in Rodriguez and Gutierrez (2003). Noteworthy, the effect of carbon partitioning on yield stress and strain hardening is captured by the approach, so that electron probe micro analyzer (EPMA) was deployed to investigate the distribution of carbon. For validation purposes, a virtual tensile test was performed on the RVE, and the effective flow curve satisfactorily matched the experimentally determined tensile test result. Thus, the individual flow curves were assumed to be valid for the material.

After the derivation of individual flow curves, the RVE is loaded under uniaxial, equibiaxial and plane-strain tensile loading conditions. In all these simulations, reaching the ultimate tensile strength is assumed to be the indicator for damage initiation. This selection of criterion is justified with the idea that strain localization on the RVE scale will result in void formation on the specimen scale. Exemplarily, fig. 3 shows the numerically determined distribution of equivalent plastic strain in the RVE loaded under uniaxial tension. White areas indicate martensite, while all other color-coded areas belong to ferrite. The strain distribution is presented for the instant when the RVE´s ultimate tensile strength was reached. It becomes obvious that there is severe strain localization in the small ferritic region in a neighbor situation with two different martensite islands. These are rather close to each other due to the small diameter of the ferritic grain. It can be expected that such extensive straining will result in the formation of a cavity, and this is exactly in line with the experimental findings presented above. Therefore it is concluded that the RVE´s effective equivalent plastic strain and stress triaxiality at that loading instant make up one point on the MBW model´s damage initiation locus. Here it is to be noted that Bai and Wierzbicki (2008) pointed out a simple relationship between stress triaxiality and normalized Lode angle valid for plane stress conditions. Likewise, the 3D-DIL can be translated into a 2D-criterion for plane stress conditions.

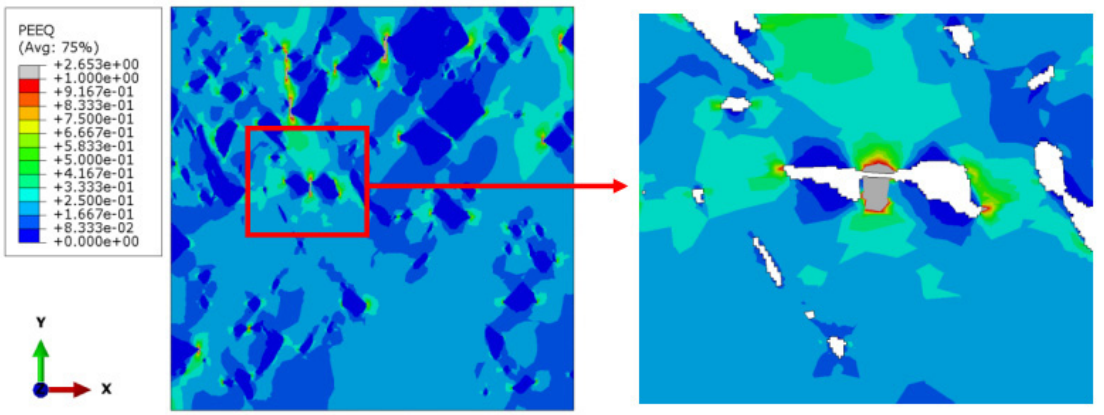

Fig. 3. Distribution of equivalent plastic strain for the instant that the RVE´s ultimate tensile stress is reached under uniaxial tensile loading condition.

The RVE simulation of plane strain and equibiaxial tensile loading conditions allowed for similar findings, but the corresponding state of stress was modified. Thus, the influence of the state of stress on damage initiation could be expressed, and additionally, the plane-stress damage initiation locus could be constructed based on the RVE simulations. Fig. 4. presents a comparison between the conventionally determined plane-stress DIL and the numerically derived values for the three stress states under investigation in the study presented. Obviously, there is a good agreement between the approaches.

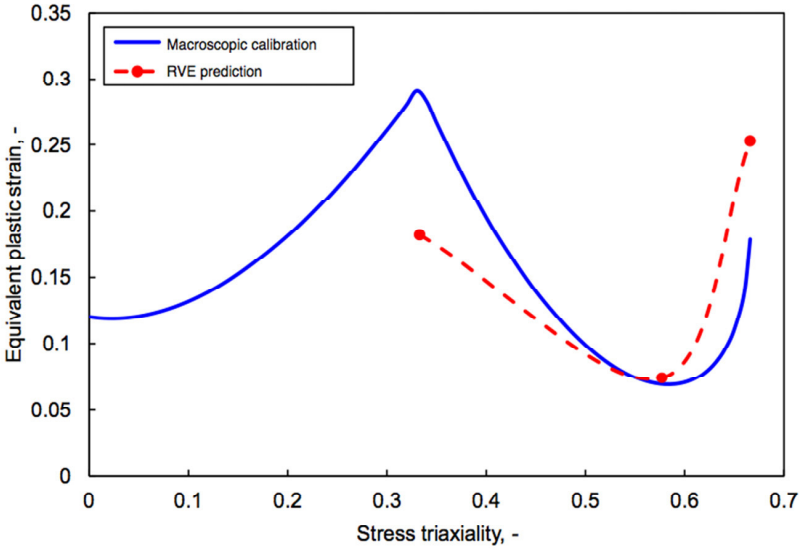

Fig. 4. Conventionally determined damage initiation locus of steel DP600 and results of RVE simulations.

3. Conclusions

- In the selected steel DP600, damage initiation mainly occurs in small ferritic grains which are in a neighbor position to two martensitic islands. Damage initiation results from extensive straining of the relatively small ferritic grain.
- The plane-stress damage initiation locus is well predicted by RVE simulations where the plastic strain localization theory is applied without any other damage criterion.

References

Bai, Y.L., Wierzbicki, T., 2008. A New Model of Metal Plasticity and Fracture with Pressure and Lode Dependence, International Journal of Plasticity 24, 1071-1096.

Barsoum, I., Faleskog, J., 2007. Rupture Mechanisms in Combined Tension and Shear—Experiments, International Journal of Solids and Structures 44, 1768-1786.

Chin-Chan, C., 1982. An investigation of the strain path dependence of the forming limit curve. International Journal of Solids and Structures 18, 205–215.

Gao, X., Zhang, G., Roe, C., 2009. A Study on the Effect of the Stress State on Ductile Fracture, International Journal of Damage Mechanics 19, 75-94.

Lian, J., Sharaf, M., Archie, F., Münstermann, S., 2013. A Hybrid Approach for Modelling of Plasticity and Failure Behaviour of Advanced High-Strength Steel Sheets, International Journal of Damage Mechanics 22, 188-218.

Tasan, C.C., Hoefnagels, J.P.M., ten Horn, C.H.L.J., Geers, M.G.D., 2009. Experimental analysis of strain path dependent ductile damage mechanics and forming limits. Mechanics of Materials 41, 1264-1276.

McClintock, F.A., 1968. A Criterion for Ductile Fracture by Growth of Holes, Journal of Applied Mechanics 35, 363-371.

Rice, J.R., Tracey, D.M., 1969. On Ductile Enlargement of Voids in Triaxial Stress Fields, Journal of the Mechanics and Physics of Solids 17, 201-217.

Rodriguez, R., Gutierrez, I., 2003. Unified formulation to predict the tensile curves of steels with different microstructures, in: T. Chandra, J.M. Torralba, T. Sakai (Eds.) Thermec'2003, Pts 1-5, Trans Tech Publications Ltd, Zurich-Uetikon, 4525-4530.